5. Results

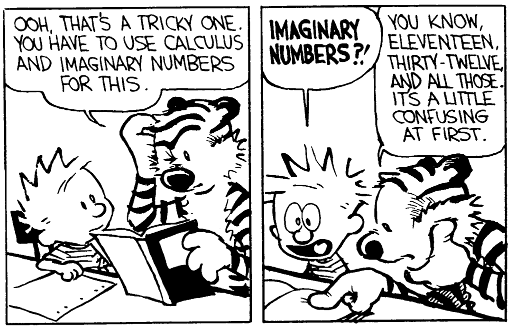

Outline

This chapter describes the recording and analysis of data from COAST. The results of the tests on astronomical objects and internal calibration sources are shown.

5.1 Visibility measurement

The aim of COAST is to measure the coherence of light from an astronomical object on a number of baselines together with a closure phase. This is done by simultaneously measuring the visibility of fringes produced from different pairs of telescopes. The visibility of the fringes is determined by how well resolved the source is on that baseline. This together with the size of the baseline measures the angular diameter of the source. However the visibility of the fringes is also reduced by the effects of atmosphere turbulence, which reduce the coherence across the finite telescope aperture. The visibility is also reduced by miss-alignments of the optics which might introduce phase tilts between the beams from each telescope. These effects can be reduced if an unresolved (point) source is observed with the target source.

This calibration source would be a small or distant star of similar brightness to the object. Care must be taken that the calibration source is not to a binary system.. This object must be also close to the target so that the light passes through a similar air path. The observing strategy would probably be to observe the calibrator, then the star and return to the calibrator. If a resolved star of known diameter is also available this could be observed to provide an extra check. The time between observations of source and calibrator is a compromise, switching rapidly between the objects wastes observing time while the telescopes move. A long delay between observations allows the atmosphere to change and reduce the effectiveness of the calibration. Based on experience with observations on the WHT a measurement of a few minutes on each object will probably be used.

5.2 COAST Status

At the time of writing, the construction of COAST is almost completed. Three out of the four telescopes are operational and the final one is currently being aligned and tested. The visible and infrared systems are both able to measure fringes on astronomical targets regularly. However the acquisition and guiding systems are not totally tuned so that finding stars still requires some work. This makes it impossible to acquire an astronomical target and then a calibration object quickly and reliably enough to make accurate diameter measurements. The test observations produced in this chapter generally used most of the night to find and observe each star. The separate computer systems controlling the trolley position, the visible and infrared cameras and the data analysis are integrated but not fully tested.

5.3 Astronomical observations

As the path trolleys sweep a fringe pattern past the detector the camera system measures the power in each of the four output beams of the correlator. Effects common to all the telescopes such as scintillation can be removed by subtracting pairs of output beams. If the correct combinations of outputs are chosen the fringe packets will add together while the scintillation is removed. However, there may be difference in efficiency of the pixels measuring each output, or a miss-alignment which reduces the signal in some pixels. To avoid this effect, the data is re-scaled before being subtracted. The final scaled difference of two outputs, N_{diff} is given by:

$$N_{diff} = N_A - N_B \frac{\langle N_A \rangle}{\langle N_B \rangle} + 2\langle N_A \rangle$$

Where $\langle N_i \rangle$ is the time averaged signal on output *i*.

The observations below were obtained on α Lyr (Vega) on 21st August 1995 in the J band, using two telescopes and two outputs of the beam combiner. Using only two outputs reduces the data taking and analysis while still allowing atmospheric scintillation to be removed. The exposure time was 1 millisecond and the full telescope aperture of 0.4 m was used.

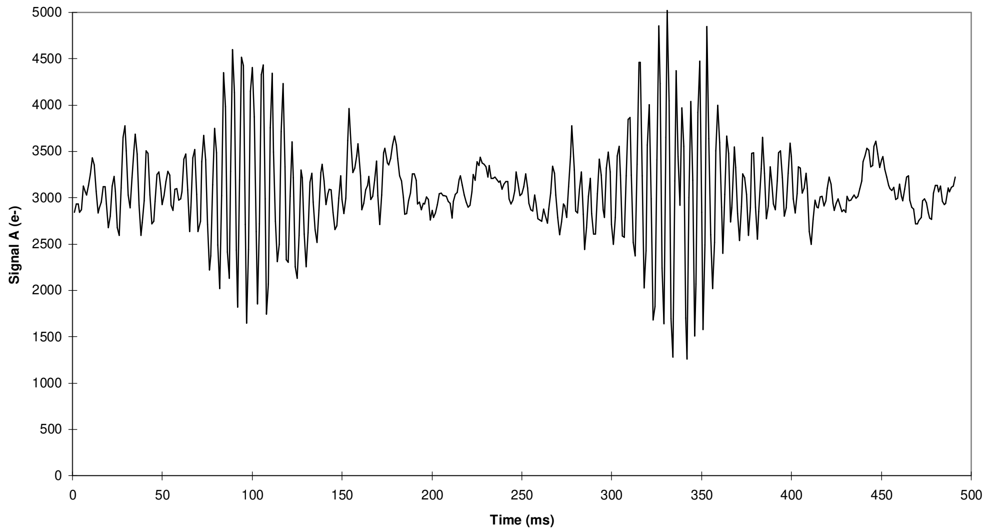

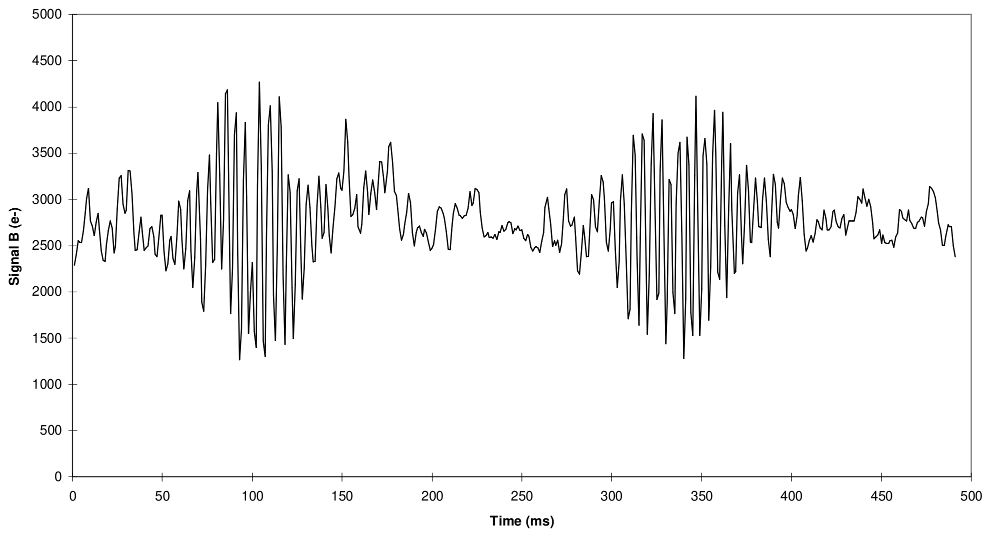

Figure 5.1: Fringes from α Lyr

The difference signal is produced by subtracting the scaled outputs as described above.

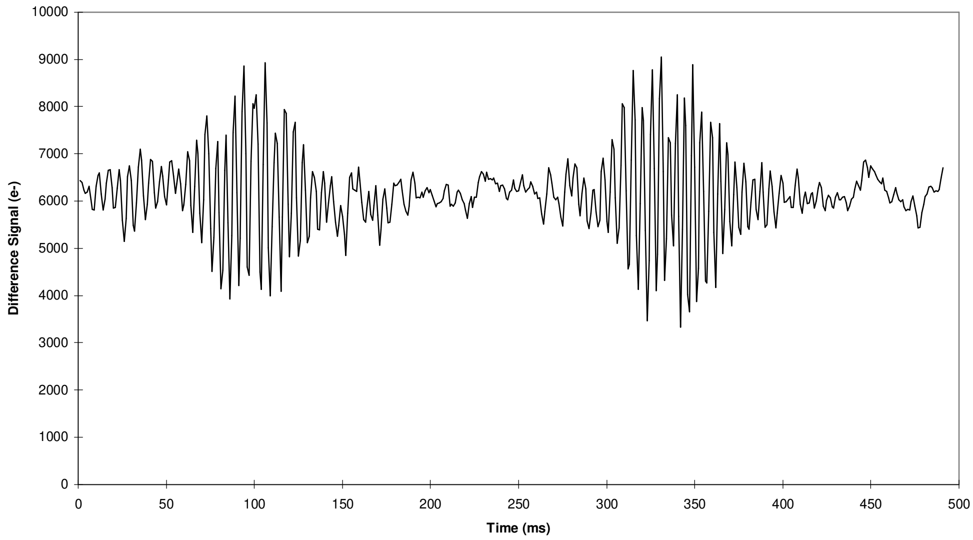

Figure 5.2: Subtracted fringe pattern

The filter bandpass is square which produces the sidelobes visible in the fringe pattern. The mean signal in Figure 5.1 is around 2500 e^-. This is about 100 times the expected read noise in each exposure and so fringes would be easily visible in the signal from a 5^{th} magnitude object.

The instantaneous visibility can be calculated of the fringes in this packet is then given by :

$$V = \frac{|N - \langle N \rangle|}{\langle N \rangle}$$

This is shown in Figure 5.3 below. The maximum visibility is about 50%, the model discussed in chapter 4 predicts that the recorded visibility from this unresolved source should be 70%. Tests with an internal source produced fringes with a maximum visibility of around 70%, the loss in visibility is probably due to miss-alignment of the optical components. This suggests that the maximum visibility of stellar fringes would be 0.7 * 0.7 which is approximately 50%, as shown in Figure 5.3.

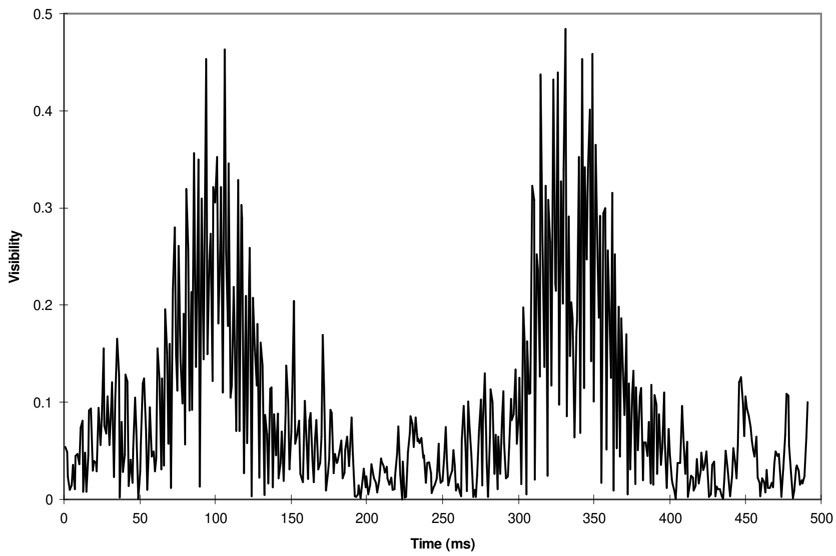

Figure 5.3: Fringe visibility

The fringe visibility in a real observation is not calculated directly but is compared to observations of a calibration source. The difference between two outputs is calculated as above. The data is then split into individual fringe envelopes. Each packet is Fourier transformed and the mean of the set of transforms found. There is a peak in the transform at the frequency of the path trolley scan. The ratio of the power in this peaks from the target and calibrator then gives the visibility.

The plot below shows a FFT of the data in Figure 5.2 produced by windowing the data as described above. The trolley is set to scan at 200 Hz and forms the main peak in the data. The atmosphere contributes power on timescales upto about 100 Hz.

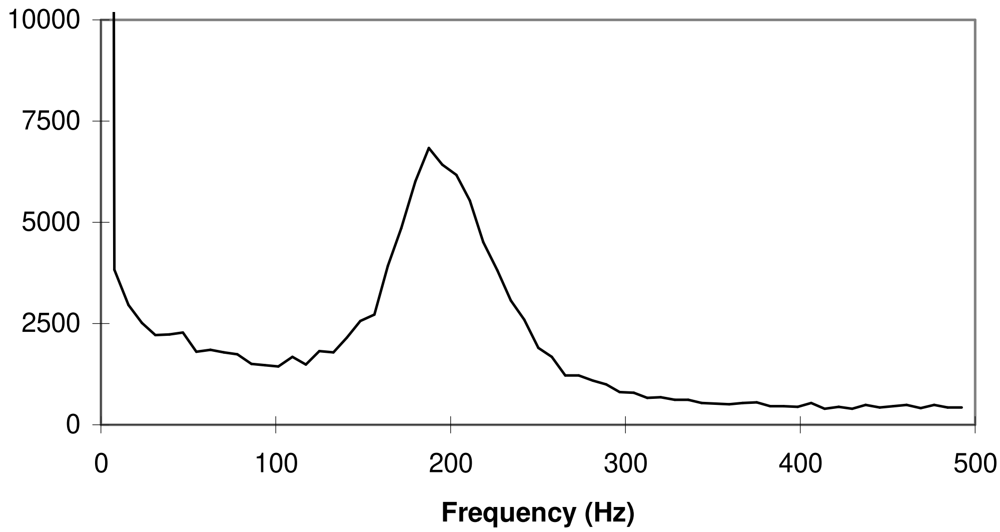

Figure 5.4: Power spectrum of α Lyr fringes

The fringe scanning speed is chosen to be high enough that the fringe frequency is above the atmospheric noise but low enough that the fringes can be adequately sampled at a reasonable camera frame rate. Ultimately with four telescopes in operation there will be six equally spaced peaks in the power spectrum, corresponding to six baselines. The scanning frequencies must be chosen so that these peaks are well separated.

5.4 Internal calibration

As described in chapter 4 it is possible to form fringes without observing an astronomical object. If a collimated beam of light is directed along one of the outputs of the beam combiner back into the system it will emerge at each telescope. The telescopes can be steered to reflect this light back into the optical system where it will form fringes. Since the light does not pass through a large part of the atmosphere the fringe visibility is generally much higher than on a star.

The plots below shows a sample of data with fringes formed on all the baselines from the three telescopes available at the time. The path compensation trolley for one telescope beam is fixed, the other two scan in a sawtooth pattern with one trolley moving at twice the speed of the other. This produces fringes from different baselines at different frequencies and so the signal from each pair of telescopes can be independently measured. This effect can be seen clearly in the transform of the fringe data.

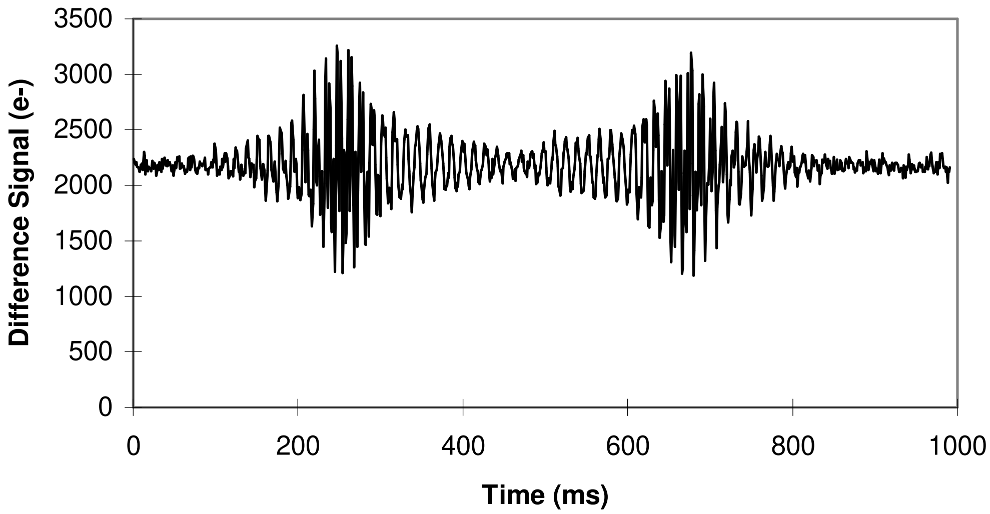

Figure 5.5: Internal fringes formed on 3 baselines

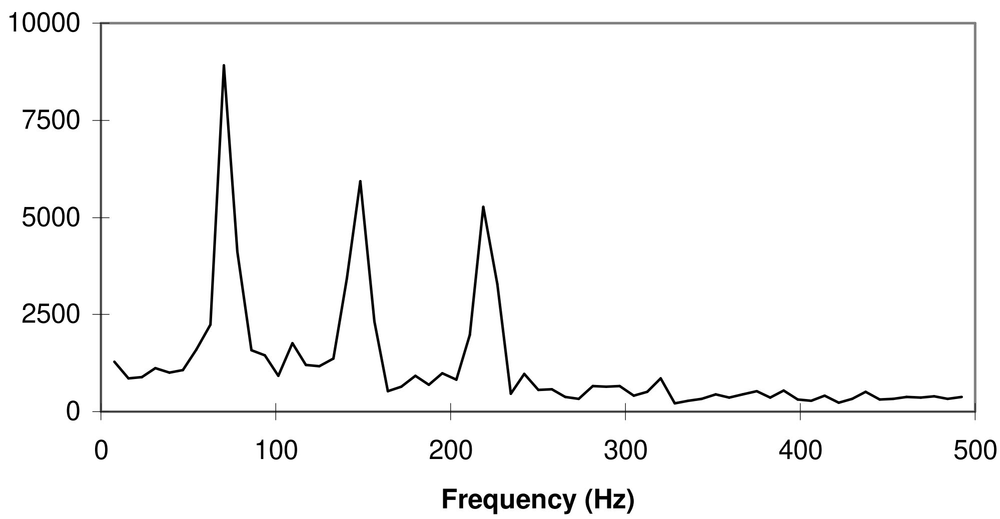

Figure 5.6: Power spectrum of 3 baseline fringes

5.5 Conclusion

This chapter has shown the data taken by the COAST infrared system. At the time of writing the telescope can take infrared measurements as regularly and reliably as the existing visible system. The astronomical data taken so far has been limited by time and weather, but the data obtained suggests that great things are possible for the future.